A Model for 4-Aminopyridine Action on K Channels: Similarities to Tetraethylammonium Ion Action

Clay M. Armstrong and Andrey Loboda
Department of Physiology, University of Pennsylvania School of Medicine, Philadelphia, Pennsylvania 19104 USA

ABSTRACT We present a model for the action of 4-aminopyridine (4AP) on K channels. The model is closely based on the gating current studies of the preceding paper and has been extended to account for ionic current data in the literature. We propose that 4AP, like tetraethylammonium ion and other quaternary ammonium ions, enters and leaves the channel only when the activation gate is open, a proposal that is strongly supported by the literature. Once in the open channel, 4AP's major action is to bias the activation gate toward the closed conformation by approximately the energy of a hydrogen bond. S4 segment movement, as reflected in gating currents, is almost normal for a 4AP-occupied channel; only the final opening transition is affected. The model is qualitatively the same as the one used for many years to explain the action of quaternary ammonium ions.

INTRODUCTION

4-Aminopyridine (4AP) is a K channel blocker that is useful clinically, particularly in the symptomatic treatment of multiple sclerosis (Bever et al., 1996; Fujuhara and Miyoshi, 1998; Smith et al., 2000). Despite its long history and its clinical usefulness, the precise mechanism of action of 4AP has for many years resisted final definition. In the preceding paper it was shown that 4AP hinders the final step in the activation sequence of nonconducting mutant K channels, without altering the preceding transitions. These observations, together with several excellent papers in the literature (Kirsch and Narahashi, 1983; Kirsch et al., 1986, 1993; Kirsch and Drewe, 1993; McCormack et al., 1994) suggested to us a model for 4AP action in conducting K channels. The model is extremely simple. It postulates that 4AP enters and leaves a channel only when the channel gate is open and that once in the channel, its only important action is to strongly bias the final transition toward the closed state. We show here that the model can explain all of the phenomena in the recent electrophysiological literature and provides an explanation for the slow kinetics of block even when 4AP is present at millimolar concentration.

In more physical terms, we imagine that 4AP occupies the (presumed) *Shaker* equivalent of the cavity seen in the KcsA channel (Doyle et al., 1998), a large dilatation of the channel internal to the selectivity filter. Once in the cavity 4AP strongly promotes the gate-closed conformation, just the opposite of tetraethylammonium ion (TEA^+) derivatives and some other ions that are known to favor the gate-open conformation.

Received for publication 23 January 2001 and in final form 23 April 2001.

Address reprint requests to Dr. Clay M. Armstrong, Department of Physiology, University of Pennsylvania School of Medicine, B-701 Richards Building, Philadelphia, PA 19104-6085. Tel.: 215-898-7816; Fax: 215-573-5851; E-mail: carmstro@mail.med.upenn.edu.

0006-3495/01/08/895/10 $2.00

EXPERIMENTAL BASIS OF THE MODEL

Gating current results cited are from the preceding paper (Loboda and Armstrong, 2001), whereas ionic current results are based primarily on the papers by McCormack et al. (1994) and two papers by Kirsch and co-workers (1986, 1993). The following list summarizes our conclusions from these results. 1) 4AP blocks the final transition in nonconducting K channels studied by gating current measurements (Loboda and Armstrong, 2001). 2) When first applied, 4 AP enters and blocks K channels with kinetics that suggest the K channels must be fully activated before 4AP can enter (McCormack et al., 1994). 3) The steady-state level of 4AP block is deepest near −40 mV where about half of the channels are open (McCormack et al., 1994). 4) Block can be partially relieved by large depolarizations (Kirsch et al., 1986; McCormack et al., 1994). 5) Restoration of block (after a large depolarization) is very slow at −100 mV and speeds up along a curve similar in position and shape to the *g-V* curve (Kirsch et al., 1986). 6) At 10 mM, 4AP decreases single-channel conductance only slightly (McCormack et al., 1994). This shows that 4AP blocks conduction through the channel, but affinity of the open channel for 4AP is very low. 7) Single-channel lifetime is decreased by 4AP at millimolar concentration (McCormack et al., 1994). This suggests that after entering a channel, 4AP induces the channel to close. 8) At −40 mV, 0.1 mM 4AP blocks I_K in *Shaker* almost completely, showing that 4AP affinity for some closed state of the channel is very high (McCormack et al., 1994).

The model

Based on the experimental results given above, we propose the following model, an extension of Scheme 1 in the preceding paper (Loboda and Armstrong, 2001).

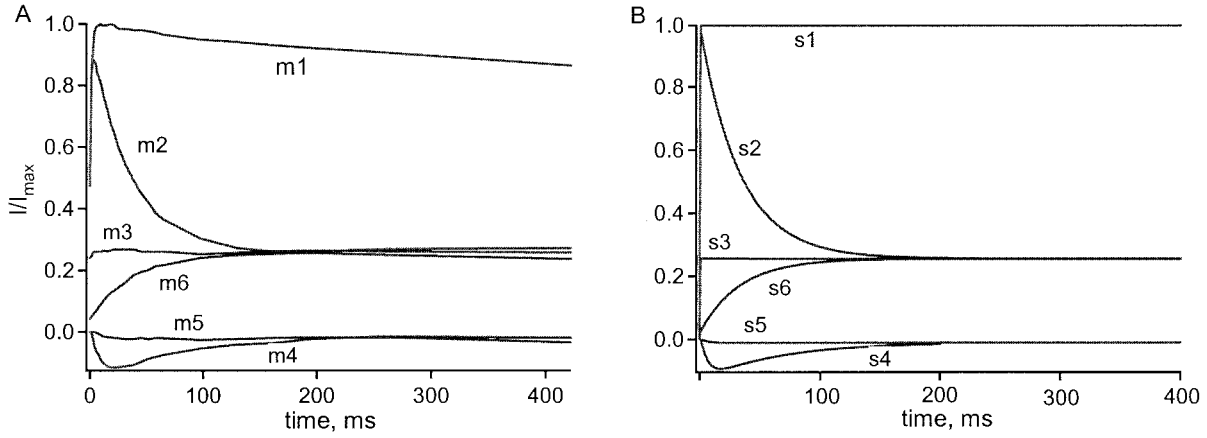

FIGURE 1 (*A*) Ionic current traces in 4AP, taken from Fig. 1 *B* of McCormack et al. (1994); (*B*) Simulations of the current traces produced with the Scheme AP in the text.

$$C_0 \underset{\beta_0}{\overset{\alpha_0}{\rightleftarrows}} C_1 \underset{\beta_1}{\overset{\alpha_1}{\rightleftarrows}} C_2 \underset{\beta_2}{\overset{\alpha_2}{\rightleftarrows}} C_3 \underset{\beta_3}{\overset{\alpha_3}{\rightleftarrows}} C_4 \underset{\beta_4}{\overset{\alpha_4}{\rightleftarrows}} C_5 \underset{\beta_5}{\overset{\alpha_5}{\rightleftarrows}} C_6 \underset{\beta_6}{\overset{\alpha_6}{\rightleftarrows}} O$$

$$\lambda \uparrow\downarrow \kappa$$

$$C_{0ap} \underset{\beta_{0ap}}{\overset{\alpha_{0ap}}{\rightleftarrows}} C_{1ap} \underset{\beta_{1ap}}{\overset{\alpha_{1ap}}{\rightleftarrows}} C_{2ap} \underset{\beta_{2ap}}{\overset{\alpha_{2ap}}{\rightleftarrows}} C_{3ap} \underset{\beta_{3ap}}{\overset{\alpha_{3ap}}{\rightleftarrows}} C_{4ap} \underset{\beta_{4ap}}{\overset{\alpha_{4ap}}{\rightleftarrows}} C_{5ap} \underset{\beta_{5ap}}{\overset{\alpha_{5ap}}{\rightleftarrows}} C_{6ap} \underset{\beta_{6ap}}{\overset{\alpha_{6ap}}{\rightleftarrows}} O_{ap}$$

(Scheme AP)

The rate constants for entry and exit of 4AP into and from the channel are $\kappa = [4AP] \times \kappa_0 \exp(0.45e_0 \times V_m/26)$, and $\lambda = 0.75\ \mu s^{-1}$ (very fast), as explained below. Entry and exit occur only when the gate is open (states O, conducting, and O_{ap}, gate open but 4AP occluded). The top row of states represent the (somewhat simplified) activation sequence of a normal channel in the absence of 4AP, and are taken without change of any of the rate constants from Scheme 1 of the preceding paper. C_0 through C_6 are closed states, and O is the conducting state, or the fully activated state in nonconducting mutants. The states in the lower row are identical except that 1) 4AP is bound in the channel and 2) state O_{ap} is not conducting although the channel gate is open: 4AP blocks conduction by its presence in the cavity. The rate constants of the lower row of transitions are identical to the ones in the upper row except for the last transition, $C_{6ap} \leftrightarrow O_{ap}$, which is strongly biased to the left by the presence of 4AP. Biasing the $C_{6ap} \leftrightarrow O_{ap}$ transition and blocking conduction through the gate-open channel are the only actions of 4AP, and the former is by far the more important, as emphasized by the heavy arrow.

4AP enters and leaves the channel only from the cytoplasm (Kirsch and Narahashi, 1983; Kirsch and Drewe, 1993) when the activation gate is open. As noted, the affinity of the open channel for 4AP is very low, so κ, which is proportional to [4AP], is small compared with λ even at 10 mM 4AP. The result is that 10 mM 4AP reduces single-channel current by only ~15% (McCormack et al., 1994). κ (and/or λ) is slightly voltage dependent, as is also the case for TEA^+ binding to a K channel. The time constant of 4AP equilibration with open channels is assumed to be diffusion limited and thus effectively instantaneous.

RESULTS

This model was fit to the results of McCormack et al. (1994) and Kirsch et al. (1986) in a series of simulations. To avoid confusion, figures from McCormack et al. (1994) will be referred to as Fig. M1, M2, etc; Fig K1, K2, etc. for Kirsch et al. (1986); and Fig. 1, 2, etc. for our figures. Similarly, their traces will be called trace m1 and trace k1, respectively, and ours will be called trace s1 (simulation 1), etc. All rate constants used in the simulations were calculated from Scheme 1 in the preceding paper and are given in Table 1. For each simulation, we describe the experimental result, interpret it in terms of the model, and give details of the simulation.

I_K in the absence of 4AP (s1)

I_K at +50 mV (taken from Fig. M1B) was fit using the scheme above with ($\kappa = 0$). In this case channels are confined to the upper row in the state diagram ($\kappa = 0$). Rate constants for the simulation were taken without alteration from the preceding paper. The only adjustment required was a 4-mV shift of the rate constant functions (54 mV in Loboda and Armstrong ≡ 50 mV in McCormack et al., −36 mV ≡ −40 mV, etc.). The original trace is m1 in Fig. 1 *A*, and the result, s1, is shown in Fig. 1 *B*. The main discrepancy between the fit and the data (trace m1) is a droop caused presumably by C-type inactivation, which was not included in our model.

Block by 4AP on initial exposure (s2)

The first depolarization soon after adding 100 μM 4AP to the bath is given by trace m2 in Fig. 1 *A* (from Fig. M1B). It shows the initial opening of the channels, none of which are 4AP-occupied at the instant of depolarization, followed by the decline of current as 4AP interacts with the channels. Trace m2 is simulated by s2 (Fig. 1 *B*), which assumes that all channels start in states C_0 through C_6 with a distribution appropriate for V_m (membrane voltage) equal to −100 mV (i.e., most channels are in C_0 and C_1). Rates α_{0-6} and β_{0-6} are the same as in s1. Rates $\alpha_{0ap\text{-}5ap}$ and $\beta_{0ap\text{-}5ap}$ are equal, respectively, to rates α_{0-5} and β_{0-5} here and in all simulations. λ was set arbitrarily to a very large value, to simulate very rapid dissociation of 4AP from the open channel ($\lambda = 0.75\ \mu s^{-1}$). κ was then set according to the formula given above (just below Scheme AP). In this formula, 0.45 is a factor to express the voltage dependence of 4AP binding, e_0 is one electronic charge, V_m is in mV, and 26 meV is kT. κ_0 (the value of κ at 0 mV) was chosen to give a K_{Dopen} of 56.7 mM, corresponding to 15% block of the open channels at 10 mM 4AP, 0 mV, based on the single-channel data of McCormack et al. (1994) that is discussed below. (Note that K_{Dopen} is for the reaction of 4AP with the open channel; it has only an indirect relation to the total fraction of the channels that are 4AP occupied.) Making λ smaller by a factor of 10 had no effect on the calculation as long as the κ/λ ratio was maintained. κ is somewhat voltage dependent, compatible with the idea that external K^+ tends to drive 4AP out of the channel. Demo and Yellen (1991) used a similar factor (0.62 rather than 0.45) to express the voltage dependence of quaternary ammonium (QA) knockout by external K^+. The voltage dependence could equally well have been attributed to λ; because equilibration is instantaneous, it makes no difference.

The time course and extent of current decay in s2 were then fit by adjusting rates α_{6ap} and β_{6ap}. A good fit required that $\alpha_{6ap} = \alpha_6/1300$, and $\beta_{6ap} = 100\ \beta_6$, as given in Table 1. This means that relative to the $C_6 \leftrightarrow O$ transition, the equilibrium constant for $C_{6ap} \leftrightarrow O_{6ap}$ is biased toward the gate-closed state C_{6ap} by a factor of 130,000. This corresponds to a bias equivalent to the energy of a strong hydrogen bond. There is a small discrepancy between data and fit, in that the simulated peak is too high. We could easily correct this, but for simplicity and clarity, and because we were surprised and pleased by the quality of the fit to data from other labs and preparations, we have not done so.

Summary

For this depolarization to +50 mV, the channels begin from their resting distribution in the unblocked states (mainly C_0 and C_1). The channels open, and at peak current, ~85% of the channels are in O, with ~0.4% in O_{ap} (equilibration between the two states is virtually instantaneous). The current declines as channels migrate from O to C_{6ap} via O_{ap}. The decline is slow (τ = 36ms) in part because the occupancy of O_{ap} is never very high, a consequence of the low affinity of the open state for 4-AP. At concentrations of 4AP that are small compared with K_{Dopen}, the decay rate of the current is a linear function of [4AP]. Most of the channels are trapped in C_{6ap} because the equilibrium of the $C_{6ap} \leftrightarrow O_{ap}$ transition is strongly biased toward C_{6ap}. Thus, at the end of the pulse, O is ~25%, O_{ap} is 0.1%, and C_{6ap} is ~75%. In our physical model, this means that ~75% of the channels have a 4AP-occupied cavity that has induced the closing of their activation gates. Note that experimentally this trace can be seen only once each time 4AP is applied, during the first pulse after the application of 4AP. As soon as some channels are 4AP-occupied, it is impossible to clear all of them unless 4AP is washed away.

Repolarizing when channels are 4-AP equilibrated (s2a, not illustrated)

At the end of s2 (the simulated pulse to +50 mV) we simulated repolarization to −100 mV for 500 ms. The channels close very quickly in this case, and there is no significant redistribution of channels between 4AP-occupied and non-occupied states. Thus, of the ~25% of channels in state O, essentially all go to unoccupied closed states (mainly C_0 and C_1). Of the ~75% that are in state C_{6ap}, virtually all go to state C_{0ap} and C_{1ap}. This simulation is not illustrated.

Depolarizing when many channels contain 4AP (s3)

Trace m3 (from Fig. M1B) shows the current during a second pulse to +50 mV, after the channels were equilibrated with 4AP during the first pulse to the same voltage (trace m2). In the interval between pulses, V_m was held at −100 mV for ~1 min. Channels that were not blocked at the end of the first pulse (~25%) open with the same time course as the unblocked channels in trace m2. This is simulated by s3, for which the rate constants were exactly the same as for s2, but with initial occupancies taken from the final values obtained from simulation 2a. We assumed there were no occupancy changes during the remaining 59.5 s at −100 mV. The success of this simulation makes it clear that the assumption is correct and that occupancy changes very slowly when all of the channel gates are closed, in agreement with the conclusions of Kirsch and Drewe (1993) that 4AP cannot leave a channel whose gate is closed. In terms of the

model, the channels at −100 mV very rarely visit the open states (O and O_{ap}) where 4AP entry and exit can occur.

This simulation also provides an explanation for the observations in Fig. M3A of McCormack et al. (1994). This figure shows that the activation time course of the current with 4AP-equilibrated channels is identical to that of channels in the absence of 4AP; the current at every point is smaller in magnitude by the same factor, exactly as in traces m1 and m3 (and simulations s1 and s3). The explanation in terms of our model is very simple: the ~25% of the channels that are in states C_0 and C_1 open with a normal time course to state O, because 4AP affects only the channels that it occupies. The ~75% in states C_{0ap} and C_{1ap} activate to state C_{6ap}. Because this is the equilibrium level for a pulse to +50 mV (O ~25%, O_{ap} ~0.1%, C_{6ap} ~75%; see s2 and s3), nothing else happens; there is no increase or decrease in the level of 4AP occupancy.

Deepening block with a small depolarization (s4)

After trace m3, McCormack et al. (1994) returned V_m to −100 mV for ~1 min and then stepped to −40 mV to produce trace m4. The current rises in magnitude as the ~25% of the channels that were not blocked at the end of trace m3 open and conduct (current is inward because of 138 mM K^+ in the external medium). Current then declines as most of these channels become 4AP-occupied.

Why is 4AP occupancy higher at −40 mV? 4AP enters an open channel and then induces it to close; i.e., 4AP biases the $C_{6ap} \leftrightarrow O_{ap}$ transition strongly to the left. The model assumes that the $C_{6ap} \leftrightarrow O_{ap}$ transition retains normal voltage dependence despite the bias: more positive voltage favors an open gate, more negative a closed gate. The result is that 4AP-occupied channels at −40 mV find it more difficult to open and release 4AP than they do at +50 mV. Numerically, the equilibrium constant for the $C_{6ap} \leftrightarrow O_{ap}$ transition favors C_{6ap} by a factor of 614 at +50 mV, increasing to a factor of 7630 at −40 mV. The equilibration rate at −40 mV is significantly slower than at +50 mV, because a larger fraction of the channels are initially retained in the closed states and fewer reach state O.

Simulation s4 resembles trace m4 fairly closely, using the rate constants given in Table 1. Rates α_0 to α_6 were calculated from Scheme 1 of Loboda and Armstrong (2001) with the 4-mV shift noted above. Rate $\alpha_{6ap} = \alpha_6/1300$ and $\beta_{6ap} = \beta_6 \times 100$, reflecting the same 4AP-induced bias noted at +50 mV (see above). In other words, the presence of 4AP in the channel biases the transition toward the gate-closed state but leaves the voltage dependence of the transition unchanged. As noted in the table, κ changes from s2 to s4, because of the voltage dependence assigned to K_{Dopen}.

A small depolarization when most channels are 4AP-occupied (s5)

At the end of trace m4, when nearly all of the channels were 4AP-occupied (in state C_{6ap}), V_m was returned to −100 mV for ~1 min. This put virtually all the channels into states C_{0ap} or C_{1ap}, and the small fraction that are not 4AP-occupied are mainly in C_0 and C_1. The channels remained in these states at −100 mV until V_m was stepped to −40 mV, resulting in trace m5. The small fraction of channels that did not contain 4AP opened to produce a low, maintained level of current, the equilibrium level for channels at −40 mV. These events are simulated in s5. We first calculated a return to −100 mV for 500 ms after s4, assumed no occupancy changes for the next ~59.5 s at −100 mV, and then calculated the s5 trace at −40 mV, using the rate constants appropriate for −40 mV (Table 1). The low, maintained current adequately reproduces the experimental trace.

Partial relief of block by a large depolarization

After trace m5 McCormack et al. (1994) returned V_m to −100 mV for ~1 min and then stepped to +50 mV to produce trace m6. At the beginning of this step virtually all of the channels are 4AP-occupied and in states C_{0ap} or C_{1ap}. As a result, the quickly rising component of current, due to channels opening from unblocked closed states, is almost inappreciable. The very small quick rise is followed by a slow rise as 4AP-occupied channels are reluctantly forced open. The equilibrium level of the current is (almost) the same as for the preceding steps to +50 mV (traces m2 and m3). Trace s6 simulates this well, using the rate constants appropriate for +50 mV. The initial occupancies were the same as for s5; i.e., almost all channels were in states C_{0ap} or C_{1ap}. Notice that the time constant for the rise of trace m6 (and s6) is the same as for the fall in current trace m2 (and s2), an observation that can be easily understood from the model. The time constant in both cases is approximately

$$\frac{1}{\alpha_{6ap} + \beta_{6ap}\left(\frac{\kappa}{\kappa + \lambda}\right)}.$$

Kirsch et al. (1986) also observed partial relief of block by depolarization, in their case a series of large depolarizations (Figs. K1 and K2): after a long period of rest during which block becomes maximal (see below for predictions of steady-state block as a function of voltage), they found that current amplitude during a series of pulses at 5/s grows as block is removed with each successive pulse up to 5 or 10 pulses. The maximum relief is larger if 1) pulsing is frequent and 2) holding potential in the interval between pulses is very negative. The negative

holding potential helps recovery by closing the channels so firmly that 4AP cannot enter in the interval between pulses.

Single-channel conductance (not illustrated)

Single-channel conductance at 0 mV is reduced by 4AP according to the formula

$$\gamma = \gamma_0\left(1 - \frac{[4AP]}{[4AP] + K_{Dopen}}\right),$$

where γ_0 is the single-channel conductance at 0 mV in the absence of 4AP, and K_{Dopen} is 56.7 mM at 0 mV. γ is reduced to 85% of γ_0 when [4AP] is 10 mM. At 100 μM, the reduction is negligible. This is in good agreement with the single-channel data of McCormack et al. (1994), Fig. M1 *C*.

Single-channel lifetime (not illustrated)

In Fig. M1 *C* of McCormack et al. (1994) single-channel lifetime is drastically shortened by 1 mM 4-AP and even more so by 10 mM. They find, on the other hand, that the time constants of the macroscopic I_K tails, as the channels close on repolarization, is unaffected by 100 μM 4AP (Fig. M3, *C* and *D*). This seems somewhat paradoxical but is easily explained by the model. Turning first to the single-channel currents, a conducting channel in state O can close by one of two paths in the presence of 4AP: $O \rightarrow C_{6\cdots0}$ or $O \rightarrow O_{ap} \rightarrow C_{6ap\cdots0ap}$. The net closing rate from state O is the sum of the rates for the first step of these two paths:

$$\text{net closing rate} = \underbrace{O \times \beta_6\left(1 - \frac{[4AP]}{[4AP] + K_{Dopen}}\right)}_{rate_0} + \underbrace{\frac{0 \times \beta_{6ap} \times [4AP]}{[4AP] + K_{Dopen}}}_{rate_{oap}}$$

The $O \rightarrow O_{ap}$ step has been incorporated in the rates by including the factor $[4AP]/(K_{Dopen} + [4AP])$. This implies instantaneous equilibration of 4AP with the open channel. The empirical fits illustrated above show that β_{6ap} is larger than β_6 by a factor of 100. Substituting 100 β_6 for β_{6ap} gives

$$\text{Net closing rate} = rate_O + rate_{Oap}$$

$$= rate_O + \frac{rate_O \times 100 \times [4AP]}{K_{Dopen} + [4AP]}.$$

Taking K_{Dopen} as 56.7 mM, $rate_{Oap}$ at 0 mV (the voltage of the single-channel recordings) in 10 mM 4AP is larger than $rate_O$ by a factor of 17.6, which means that ~94% of the closings are via the $O_{ap} \rightarrow C_{6ap}$ path, ~6% via the $O \rightarrow C_6$ path. The lifetime is thus determined mainly by the $O_{ap} \rightarrow C_{6ap}$ path, with the result that 94% of the observed lifetimes in the presence of 4AP are shortened by a factor of 18.6. This prediction looks acceptable in light of the limited information on lifetime available in Fig. M1 *C*.

Turning from single-channel lifetime to the macroscopic currents presented in Fig. M3, *C* and *D*, their figure (not reproduced here) shows that the tails are little affected by 100 μM 4AP, in contrast to the drastic shortening of single-channel lifetime caused by 1 and 10 mM 4AP. Calculations from the model show that in the conditions of Fig. M3, $rate_O$ is much larger than $rate_{Oap}$ because of the reduction of 4AP concentration and an increase in K_{Dopen}, which has a small voltage dependence. Overall, the net closing rate is 1.03 times faster than in the absence of 100 μM 4AP. Even if K_{Dopen} were voltage independent (which seems very unlikely) the rate would be only 1.18 times faster, a difference that would be hard to measure. Both of these numbers are slightly smaller if 4AP equilibration with the open channel is not instantaneous. Thus, single-channel lifetime is strongly reduced, whereas the closing rate as measured from the tails (at lower 4AP concentration) is almost unaffected.

Single-channel closed times

Closed times at 0 mV are much longer in 1 and 10 mM 4AP (Fig. M1 *C*). In terms of the model, reopening occurs in two ways:

$$C_6 \xrightarrow{\alpha_6} O \text{ and } C_{6ap} \xrightarrow{\alpha_{6ap}} O_{ap}$$

Because O_{ap} is in essentially instantaneous equilibrium with O, these two opening paths both result in single-channel current that is slightly reduced by rapid flickering as 4AP enters and leaves the open channel. There will thus be two populations of closings, short ones into C_6 and long ones into C_{6ap}, the latter longer by the ratio of α_6/α_{6ap}, or 1300 times. This is qualitatively compatible with the limited data in Fig. M1 *C*.

Gating currents

In the preceding paper the following scheme was shown to fit gating currents generated by W434F in the absence of 4AP:

$$\begin{array}{cccccccccccccc} & 5000 & & 7000 & & 6000 & & 4000 & & 5000 & & 6000 & & 7000 \\ & (0.2) & & (0.4) & & (0.4) & & (0.5) & & (0.4) & & (1.1) & & (0.18) \\ C_0 & \leftrightarrow & C_1 & \leftrightarrow & C_2 & \leftrightarrow & C_3 & \leftrightarrow & C_4 & \leftrightarrow & C_5 & \leftrightarrow & C_6 & \leftrightarrow & O \\ & (-0.4) & & (-0.6) & & (-0.6) & & (-0.6) & & (-0.5) & & (-0.7) & & (-0.52) \\ & 600 & & 800 & & 1200 & & 1200 & & 2000 & & 6000 & & 150 \end{array}$$

early steps intermediate final

The numbers give the forward and backward rate (s^{-1}) for each transition at 0 mV, and the numbers in parentheses give the apparent valence of the transitions. The scheme is equivalent to the upper row of states in Scheme AP, given above. To simulate 4AP action on gating currents, the last step was eliminated in the previous paper or, equivalently, biased so far toward C_6 that it does not occur significantly. The simulations of the last paper thus are sufficient to show compatibility of the model with the gating current results presented there. In 1 mM 4AP the channels are mainly in the lower row of states in Scheme AP, for which the $C_{6ap} \rightarrow O_{ap}$ transition is highly unlikely.

Steady-state block as a function of V_m

Because of the strong bias of the $C_{6ap} \leftrightarrow O_{ap}$ transition toward C_{6ap}, most of the channels are 4AP-occupied at all voltages negative to about +50 mV for a 4AP concentration of 100 μM. The bias becomes even stronger as V_m goes negative, because of the voltage dependence of the $O_{ap} \leftrightarrow C_{6ap}$ transition, and as a result block deepens as voltage goes negative. This is somewhat offset by the opposite but less strong voltage dependence of K_{Dopen}, which results in less 4AP occupancy of channels with open gates. Fig. 2 shows predicted values for steady-state 4AP occupancy at 100 μM 4AP. An important point qualitatively is that most of the channels are 4AP-occupied regardless of the holding potential.

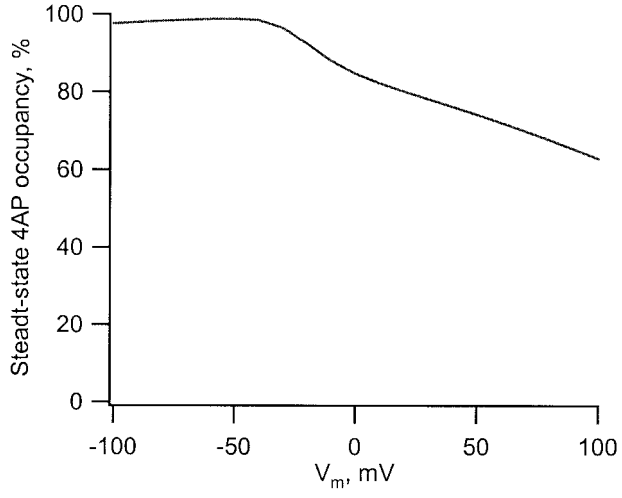

FIGURE 2 Steady-state 4AP occupancy of the channels as a function of V_m, as predicted by Scheme AP in the text.

Restoration of block: time and holding potential dependence

After prolonged exposure to 4AP, McCormack et al. (1994) cleared a certain fraction of the channels with long pulses to +100 mV and then examined the restoration of block as a function of voltage, as illustrated in Fig. 3 *A* (from Fig. M2 *A*). The protocol shown in the figure was applied continuously, with rest periods at −100 mV between applications. Note that at the end of the pulse to +100 the current is the same in all cases, indicating that the fraction of the channels cleared of 4AP was always the same both at pulse end, and also at the beginning of the following prepulse, which came in every case after a rest period of the same voltage and duration. Using the −40-mV prepulse as an example, I_K activated to ~500 pA inward and then declined as 4AP blocked many of the channels that were clear at the end of the preceding pulse to +100 mV. The fraction of channels still clear of 4AP at the end of the prepulse was conveniently measured from the initial current at +100 mV. The initial current was small, with a −40-mV prepulse where block was maximal, and grew larger as the prepulse voltage increased. After a prepulse to −60 mV, the initial current in the test pulse was very large, because few of the 4AP-free channels opened and admitted 4AP during the prepulse. During the +100-mV pulse, current usually increased as a fraction of the channels became free of 4AP, reaching a steady state after ~100 ms. This relief of block by a large pulse is the same phenomenon as in traces m6 and s6 of Fig. 1.

This experiment is simulated in Fig. 3 *B*, using the rate constants for each voltage that is given in Table 1. The model predicts that 36% of the channels are unblocked after a long pulse to +100 mV. In general, the simulation seems in good qualitative agreement with the experimental traces. The current at −40 mV increases as unblocked channels

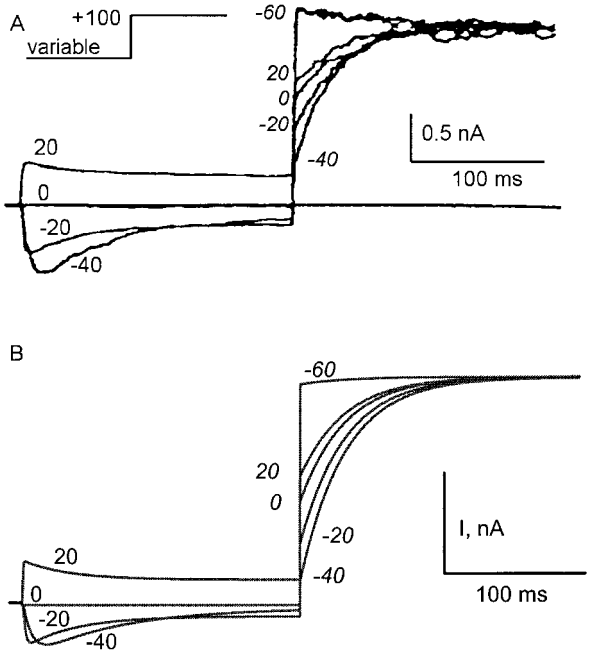

FIGURE 3 (*A*) I_K traces (taken from Fig. 2 of McCormack et al., 1994), acquired using the inset protocol. The protocol was applied repeatedly. As is evident from the current at the end of the +100-mV pulse, the same fraction of the channels was cleared of 4AP, regardless of the preceding prepulse. This fraction did not change significantly during the rest period and was thus the same at the beginning of the next prepulse, a 200-ms pulse to −60, −40, −20, 0, or +20 mV. The prepulse, during which the level of 4AP block generally changed, was followed by a pulse to +100 mV. The traces illustrate that block is slight if the activation gate is closed during the first step (−60 mV), deep for a first pulse to −40 mV, and progressively less deep as pulse voltage increases to +20 mV. (*B*) Simulations of these traces using Scheme AP in the text.

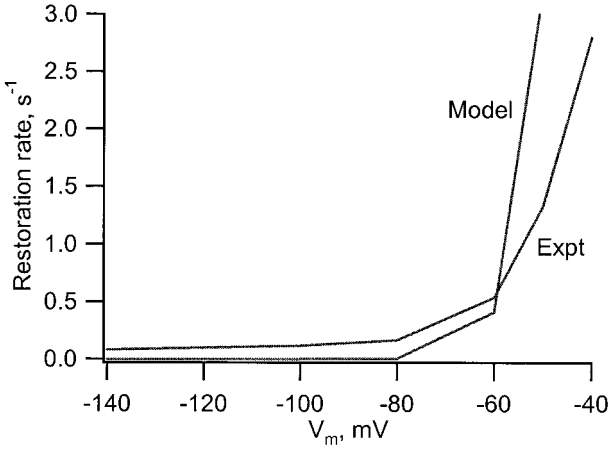

FIGURE 4 The trace labeled Expt is taken from Fig. 4 of Kirsch et al. (1986). It shows the rate of restoration of block as a function of the holding potential between test pulses. Channels were partially cleared of 4AP by a series of large pulses before the restoration measurement. The trace labeled Model is predicted by Scheme AP in the text.

activate and then decays as 4AP enters and closes them. For a prepulse to 20 mV, I_K activates more rapidly and then declines only slightly, because in the steady state at this voltage the model predicts that 20% of the channels remain unblocked. At +100 mV, current increases in all of the traces, mainly because this high voltage drives channels from C_{6ap} to O_{ap}, as in simulation s6 (Fig. 1). At +100 mV, 4AP is likely to dissociate from a channel in state O_{ap}, because K_{Dopen} is 9.4 mM according to the model, and only 100 μM 4AP is present. A slight discrepancy is that the simulated current increases slightly, rather than decaying slightly at +100 mV after the −60-mV prepulse. This could be the result of C-type inactivation.

Somewhat similar experiments had previously been performed by Kirsch et al. (1986). They found that after they cleared 4AP from a portion of the channels with a series of large pulses, the restoration rate of 4AP block, as measured by the decline of maximum I_K elicited by a test pulse, is strongly voltage dependent. Their experimental curve is given by Expt in Fig. 4 and shows the rate at which the cleared channels again become blocked. The curve indicates that if V_m is held at −140 mV after clearing a fraction of the channels with large pulses, 4AP reenters and blocks the cleared channels at a very slow rate, as determined with a test pulse. The reentry (restoration) rate grows rapidly as the holding potential is made positive to ~−80 mV. At −50 mV, the restoration rate was 1.3 s^{-1}, meaning that the cleared channels were becoming blocked again with a time constant of ~0.75s. The qualitative explanation for this curve in terms of our model is that 4AP can enter the channel only when it is open and that the open probability increases steeply with voltage near −80 mV. Predictions of the model for the restoration rate (open probability) are given by the curve labeled Model in the figure. The difference in steepness probably lies in the impossibility of measuring the true restoration rate as a function of holding potential without perturbing the system with test pulses; test pulses speed the restoration of block by opening the channels. This effect distorts the rate heavily at negative voltages where the open probability is very low. Nonetheless, there may be more block than the model predicts when a single pulse is applied after 4AP application with V_m held negative for a time with no pulsing. Possibly the channels flicker open more than predicted, or there may be a very slow entry even when channels are closed. More experiments will be required on this point.

The effect of Cs^+ and Rb^+ on block restoration rate

After clearing some channels of 4AP with a series of large depolarizing pulses at high frequency, Kirsch et al. (1986) noted that the restoration of block was slowed by the relatively impermeant ions Cs^+ (slowing factor 20)

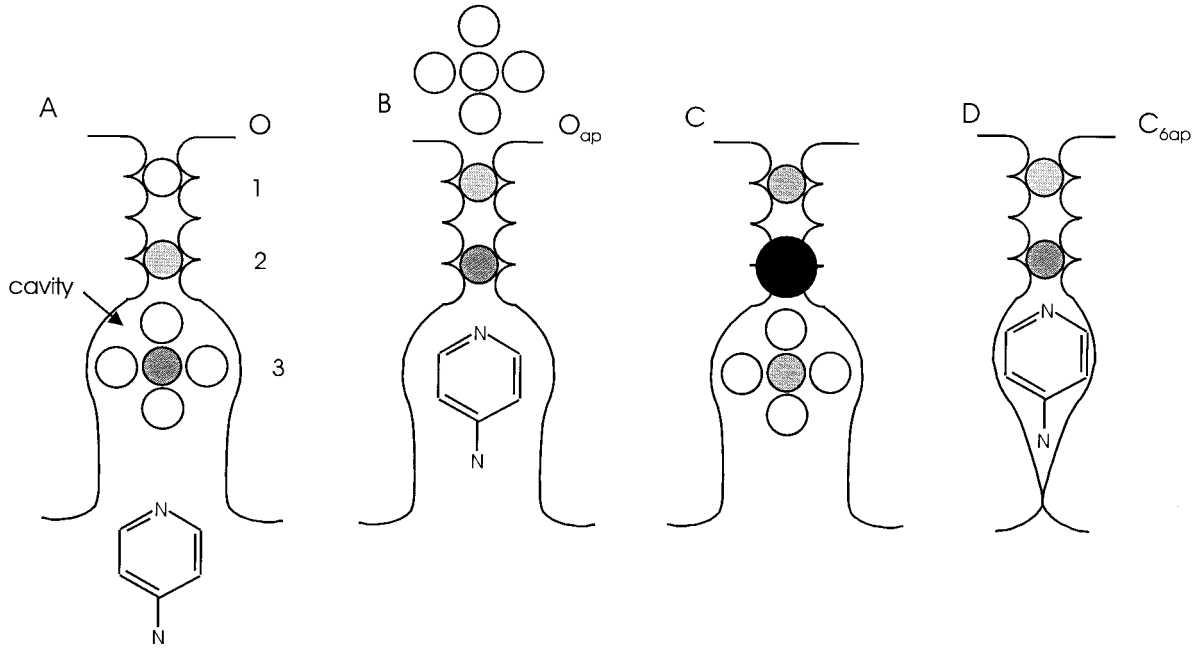

FIGURE 5 Physical models based loosely on the KcsA channel structure given by Doyle et al. (1998). *A* and *B* show the displacement of a hydrated K^+ ion (dark gray, surrounded by four white H_2O molecules) from the cavity to the selectivity filter as a 4AP molecule enters the cavity from the cytoplasm. (*C*) Displacement is less likely if a large Cs^+ ion (black) must move through the selectivity filter, making 4AP entry much slower, as found by Kirsch et al. (1986). (*D*) Occupancy of the cavity by the relatively small 4AP molecule induces closing of the channel.

and Rb^+ (3.8). "In contrast, highly permeant ions such as K^+ and highly impermeant ions such as Na^+ and tetramethylammonium ion appear to have no effect on the time course of block restoration." The time course in Cs^+ in fact has two clearly resolved components, the faster with a time course like Na^+ and a second that is 20 times slower. A possible explanation is diagramed in Fig. 5, *A–C*. To enter its blocking site (presumably the cavity), 4AP must displace all of the occupying ions one position toward the outside, as shown in Fig. 5, *A* and *B*. In Fig. 5 *A*, a K ion (dark gray) surrounded by four water molecules is in the cavity, and two dehydrated K ions (medium and light gray) are in the selectivity filter. As it enters the cavity 4AP pushes each of the occupying K ions outward and expels the light gray K^+ ion into the solution where it is rehydrated. The displacement occurs rapidly when K^+ occupies all positions, because K^+ permeates easily through the selectivity filter. When the external medium contains only impermeant ions, e.g., Na^+, or a significant amount of K^+, all positions are occupied by K^+. When the external medium contains Cs^+, a fraction of the channels will contain one or more Cs^+ ions, and the remainder will contain only K^+ ions. A Cs^+ ion occupying the cavity or, as diagramed in Fig. 5 *C*, the inner position in the selectivity filter, is hard to displace outward, because it is too large to move easily into or through the filter. The same general argument applies to the somewhat smaller Rb^+ ion.

Reoccupancy by 4AP thus proceeds rapidly in Na^+ because the channels are occupied exclusively by K^+, which is easily displaced. With Cs^+ in the external medium, reoccupancy occurs at two rates, rapidly for the K^+-occupied channels and slowly for the Cs^+-occupied channels. The slowing factor found by Kirsch et al. (1986) for Rb^+ agrees rather closely with the current-carrying ability of Rb^+ through squid K channels: Rb^+ carries about one-fourth as much current as K^+ (Bezanilla and Armstrong, 1972). In the same study, Cs^+ permeability was too small to quantitate, but Hille (1992) gives the K^+/Cs^+ permeability ratio of frog node as >13, in reasonable agreement with the $20\times$ slowing observed by Kirsch et al. (1986).

Fig. 5 *D* shows the closed state of the channel in the presence of 4AP and is discussed below.

DISCUSSION

The simulations presented above show that our model reproduces well the data in the literature regarding 4AP action on gating currents and both macroscopic and single-channel ionic currents. We discuss first evidence in the literature regarding the likelihood of the physical

TABLE 1 Rate constants employed in the simulations

	−100 mV	−60 mV	−40 mV	−20 mV	0 mV	20 mV	50 mV	100 mV
α_0, α_{0ap}	2.2480	3.095	3.749	4.399	5.162	6.057	7.698	11.48
β_0, β_{0ap}	2.972	1.567	1.067	0.775	0.562	0.408	0.252	0.113
α_1, α_{1ap}	1.413	2.680	3.935	5.418	7.462	10.277	16.608	36.96
β_1, β_{1ap}	8.849	3.376	1.898	1.174	0.762	0.449	0.218	0.0659
α_2, α_{2ap}	1.211	2.297	3.372	4.644	6.396	8.808	14.235	31.682
β_2, β_{2ap}	13.273	5.064	2.847	1.761	1.090	0.674	0.328	0.0989
α_3, α_{3ap}	0.542	1.206	1.984	2.905	4.332	6.460	11.763	31.938
β_3, β_{3ap}	13.259	5.072	2.849	1.762	1.090	0.674	0.327	0.0986
α_4, α_{4ap}	1.009	1.914	2.810	3.870	5.330	7.340	11.862	26.397
β_4, β_{4ap}	14.780	6.640	4.109	2.754	1.846	1.237	0.679	0.249
α_5, α_{5ap}	0.074	0.428	1.231	2.968	7.154	17.245	64.542	582.26
β_5, β_{5ap}	9.874	3.220	1.644	0.939	0.536	0.306	0.132	0.0326
α_6	3.407	4.544	5.401	6.238	7.204	8.320	10.325	14.799
β_6	1.200	0.522	0.317	0.209	0.138	0.0911	0.0488	0.0172
α_{6ap}	0.0026	0.0035	0.00416	0.00480	0.00554	0.00640	0.00794	0.01138
β_{6ap}	120.08	52.251	31.718	20.923	13.802	9.104	4.878	1.724
κ	0.219	0.449	0.691	0.991	1.421	2.037	3.496	8.599
λ	750	750	750	750	750	750	750	750

Rates in ms^{-1} are given for eight values of V_m.

picture employed in the model and then consider alternative kinetics models.

The physical picture

Where does 4AP bind? Kirsch and Drewe (1993) and Kirsch et al. (1993) present strong evidence that the binding site is the cytoplasmic mouth of the pore and that "a specific portion of the S6 transmembrane segment was uniquely able to enhance 4AP block with no gating change." The site may overlap with the binding site for QA ions (Kirsch et al., 1993). McCormack et al. (1994) conclude that "4-AP is likely to be in contact with all four subunits at the mouth of the pore." What controls access to this site? Kirsch and Drewe (1993) say that the site "appears to be guarded by the activation gate." McCormack et al. (1994) somewhat less explicitly say that "other portions of the protein may act as gates regulating access." Having the benefit of the work by Doyle et al. (1998), we propose that the 4AP site and the QA site are in the cavity and that the activation gate controls access for both ions.

The physical picture that emerges is a channel with a rather nonspecific binding site in the cavity that is protected by an internally located gate, precisely the same physical model that was used to explain the effects of TEA^+ and its derivatives (QA ions). There are, in fact, more similarities than differences in the action of 4AP and QA ions. Both enter their binding site from the cytoplasm, when the activation gate is open. Both can be trapped in the channel by closing of the activation gate at negative voltage. The difference in their mechanism of action is quantitative rather than qualitative. 4AP in the cavity promotes gate closing and binds stably in the channel when the activation gate is closed. QA ions and other ions usually hinder gate closing (Armstrong, 1971; Melishchuk and Armstrong, 2001), rather than facilitating it, and this is the important quantitative difference between 4AP and QA ions. An exception to this was found in the I470C mutant, where Holmgren et al. (1997) found that TEA^+ caused a slight equilibrium stabilization of the closed state. This is qualitatively similar to 4AP acting on *Shaker* or W434F, but the stabilization with 4AP is quite large, a factor of 130,000 (~7 kcal/mol). Once the gate is closed with 4AP in the channel, the S4 segments are free to move and generate almost completely normal gating current (Loboda and Armstrong, 2001). The same is true of I470C channels that trap TEA^+ inside (Melishchuk and Armstrong, 2001).

A sketch of a 4AP-occupied channel in the closed state is given in Fig. 5 *D*. 4AP is smaller than a hydrated K^+ ion, and its presence induces an inward movement of the cavity walls (mechanism unknown), which in turn closes the gate internal to the cavity. The gate is presented here as a diaphragm, as suggested by the results of Doyle et al. (1998) and del Camino et al. (2000). An alternative would be to draw the gate as a flap (Armstrong, 1971). Functionally, a diaphragm and a flap are equivalent, in that both allow or prevent access to the pore, and both can be imagined as either fully open or fully closed (normally there are no subconductance states). The closed gate traps 4AP in the cavity or, if the cavity is empty of 4AP, prevents its entry.

Alternative kinetic models

Two alternate models that illustrate useful general principles were considered in detail.

In these models, 4AP can 1) enter exclusively when the channel is in state C_6:

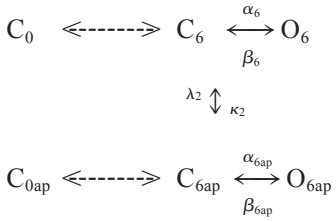

or 2) when it is either in C_6 or O:

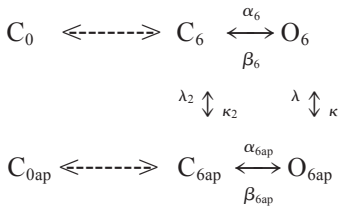

Neither of these models works in our hands. The first model cannot explain the effect of 4AP on channel lifetime or the effect of 10 mM 4AP on single-channel current. Both phenomena require that 4AP be able to enter a channel with open activation gate. Thus, we can rule out all models like the first one that lack a direct path from state O to state O_{ap}. The second model, in which 4AP can enter either in the ultimate closed state (C_6) or the open state has other problems. 1) The rising phase of trace m2 (Fig. M1 and Fig. 1) follows trace m1 quite faithfully up to ~75% of maximum current. This can happen only if κ_2 is quite small compared with rate α_6: channels in state C_6 must mainly enter state O and produce current. Very few can be bled off directly into C_{6ap}. By extension, trace m2 rules out all models in which there is significant flux from the upper to the lower row from any of the closed states: 4AP can enter and leave only when the activation gate is open. 2) The rate of block through the closed state path should decrease with voltage, as channels are sequestered ever more firmly in state O. If κ_2 is small, as required by point 1, 4AP entry by the closed state path ($C_6 \rightarrow C_{6ap}$) must be negligible at +50 mV. These two considerations seem sufficient to rule out significant 4AP entry in any of the closed states.

REFERENCES

Armstrong, C. M. 1971. Interaction of tetraethylammonium ion derivatives with the potassium channels of giant axons. *J. Gen. Physiol.* 59:413.

Bezanilla, F., and C. M. Armstrong. 1972. Negative conductance caused by entry of sodium and cesium ions into the potassium channels of squid axons. *J. Gen. Physiol.* 60:588–608.

Bever, C. T., P. A. Anderson, J. Leslie, H. S. Panitch, S. Dhib-Jalbut, O. A. Khan, R. Milo, J. R. Hebel, K. L. Conway, E. Katz, and K. P. Johnson. 1996. Treatment with oral 3,4 diaminopyridine improves leg strength in multiple sclerosis patients: results of a randomized, double-blind, placebo-controlled, crossover trial. *Neurology.* 47:1457–1462.

del Camino, D. M. Holmgren, Y. Liu, and G. Yellen. 2000. Blocker protection in the pore of a voltage-gated K^+ channel and its structural implications. *Nature.* 403:321–325.

Demo, S., and G. Yellen. 1991. The inactivation gate of the *Shaker* K^+ channel behaves like an open-channel blocker. *Neuron.* 7:743–753.

Doyle, D. A., J. M. Carbal, R. A. Pfuetzner, A. Kuo, J. M. Gullbis, S. L. Cohen, B. T. Chait, and R. M. MacKinnon. 1998. The structure of the potassium channel: molecular basis of K^+ conduction and selectivity. *Science.* 280:69–77.

Fujuhara, K., and T. Miyoshi. 1998. The effects of 4-aminopyridine on motor evoked potentials in multiple sclerosis. *J. Neurol. Sci*. 159: 102–106.

Hille, B. 1992. Ionic Channels of Excitable Membranes, 2nd ed. Sinauer, Sunderland, MA.

Holmgren, M., P. L. Smith, and G. Yellen. 1997. Trapping of organic blockers by closing of voltage-dependent K^+ channels: evidence for a trap door mechanism of activation gating. *J. Gen. Physiol.* 109:527–535.

Kirsch, G. E., and J. A. Drewe. 1993. Gating-dependent mechanism of 4-aminopyridine block in two related potassium channels. *J. Gen. Physiol.* 102:797–816

Kirsch, G. E., and T. Narahashi. 1983. Site of action and active form of aminopyridines in squid axon membranes. *J. Pharmacol. Exp. Ther.* 226:174–179.

Kirsch, G. E., C. C. Shieh, J. A. Drewe, D. F. Vener, and A. M. Brown. 1993. Segmental exchanges define 4-aminopyridine binding and the inner mouth of K^+ pores. *Neuron.* 11:503–512.

Kirsch, G. E., J. Z. Yeh, and G. S. Oxford. 1986. Modulation of aminopyridine block of potassium currents in squid axon. *Biophys. J.* 50: 637–644.

Loboda, A., and C. M. Armstrong. 2001. Resolving the gating charge movement associated with late transitions in K channel activation. *Biophys. J.* 81:905–916.

McCormack, K., W. J. Joiner, and S. H. Heinemann. 1994. A characterization of the activating structural rearrangements in voltage-dependent *Shaker* K^+ channels. *Neuron.* 12:301–315.

Melishchuk, A., and C. M. Armstrong. 2001. Mechanism underlying slow kinetics of the OFF gating current in *Shaker* potassium channel. *Biophys. J.* 80:2167–2175.

Smith, K. J., P. A. Felts, and G. R. John. 2000. Effects of 4-aminopyridine on demyelinated axons, synapses, and muscle tension. *Brain.* 123: 171–184.